terms of E_z or H_z. Doing so yields

$$E_r = -\frac{j}{q^2}\left(\beta\frac{\partial E_z}{\partial r} + \frac{\mu\omega}{r}\frac{\partial H_z}{\partial \phi}\right) \tag{2-35a}$$

$$E_\phi = -\frac{j}{q^2}\left(\frac{\beta}{r}\frac{\partial E_z}{\partial \phi} - \mu\omega\frac{\partial H_z}{\partial r}\right) \tag{2-35b}$$

$$H_r = \frac{-j}{q^2}\left(\beta\frac{\partial H_z}{\partial r} - \frac{\omega\epsilon}{r}\frac{\partial E_z}{\partial \phi}\right) \tag{2-35c}$$

$$H_\phi = \frac{-j}{q^2}\left(\frac{\beta}{r}\frac{\partial H_z}{\partial \phi} + \omega\epsilon\frac{\partial E_z}{\partial r}\right) \tag{2-35d}$$

where $q^2 = \omega^2\epsilon\mu - \beta^2 = k^2 - \beta^2$.

Substitution of Eqs. (2-35c) and (2-35d) into Eq. (2-34c) results in the wave equation in cylindrical coordinates

$$\frac{\partial^2 E_z}{\partial r^2} + \frac{1}{r}\frac{\partial E_z}{\partial r} + \frac{1}{r^2}\frac{\partial^2 E_z}{\partial \phi^2} + q^2 E_z = 0 \tag{2-36}$$

and substitution of Eqs. (2-35a) and (2-35b) into Eq. (2-33c) leads to

$$\frac{\partial^2 H_z}{\partial r^2} + \frac{1}{r}\frac{\partial H_z}{\partial r} + \frac{1}{r^2}\frac{\partial^2 H_z}{\partial \phi^2} + q^2 H_z = 0 \tag{2-37}$$

It is interesting to note that Eqs. (2-36) and (2-37) each contain either only E_z or H_z. This appears to imply that the longitudinal components of **E** and **H** are uncoupled and can be chosen arbitrarily provided that they satisfy Eqs. (2-36) and (2-37). However, in general, coupling of E_z and H_z is required by the boundary conditions of the electromagnetic field components described in Sec. 2-4-4. If the boundary conditions do not lead to coupling between the field components, mode solutions can be obtained in which either $E_z = 0$ or $H_z = 0$. When $E_z = 0$ the modes are called *transverse electric* or TE modes, and when $H_z = 0$ *transverse magnetic* or TM modes result. *Hybrid* modes exist if both E_z and H_z are nonzero. These are designated as HE or EH modes, depending on whether H_z or E_z, respectively, makes a larger contribution to the transverse field. The fact the hybrid modes are present in optical waveguides makes their analysis more complex than in the simpler case of hollow metallic waveguides where only TE and TM modes are found.

2.4.3 Wave Equations for Step-Index Fibers

We now use the above results to find the guided modes in a step-index fiber. A standard mathematical procedure for solving equations such as Eq. (2-36) is to use the separation-of-variables method, which assumes a solution of the form

$$E_z = AF_1(r)F_2(\phi)F_3(z)F_4(t) \tag{2-38}$$

As was already assumed, the time- and z-dependent factors are given by

$$F_3(z)F_4(t) = e^{j(\omega t - \beta z)} \tag{2-39}$$

since the wave is sinusoidal in time and propagates in the z direction. In addition, because of the circular symmetry of the waveguide, each field component must not change when the coordinate ϕ is increased by 2π. We thus assume a periodic function of the form

$$F_2(\phi) = e^{j\nu\phi} \tag{2-40}$$

The constant ν can be positive or negative, but it must be an integer since the fields must be periodic in ϕ with a period of 2π.

Substituting Eq. (2-40) into Eq. (2-38) the wave equation for E_z [Eq. (2-36)] becomes

$$\frac{\partial^2 F_1}{\partial r^2} + \frac{1}{r}\frac{\partial F_1}{\partial r} + \left(q^2 - \frac{\nu^2}{r^2}\right)F_1 = 0 \tag{2-41}$$

which is a well-known differential equation for Bessel functions.[24-26] An exactly identical equation can be derived for H_z.

For the configuration of the step-index fiber we consider a homogeneous core of refractive index n_1 and radius a, which is surrounded by an infinite cladding of index n_2. The reason for assuming an infinitely thick cladding is that the guided modes in the core have exponentially decaying fields outside the core which must have insignificant values at the outer boundary of the cladding. In practice, optical fibers are designed with claddings that are sufficiently thick so that the guided-mode field does not reach the outer boundary of the cladding. To get an idea of the field patterns, the electric field distributions for several of the lower-order guided modes in a symmetrical slab waveguide were shown in Fig. 2.14. The fields vary harmonically in the guiding region of refractive index n_1 and decay exponentially outside of this region.

Equation (2-41) must now be solved for the regions inside and outside the core. For the inside region the solutions for the guided modes must remain finite as $r \to 0$, whereas on the outside the solutions must decay to zero as $r \to \infty$. Thus for $r < a$ the solutions are Bessel functions of the first kind of order ν. For these functions we use the common designation $J_\nu(ur)$. Here $u^2 = k_1^2 - \beta^2$ with $k_1 = 2\pi n_1/\lambda$. The expressions for E_z and H_z inside the core are thus

$$E_z(r < a) = AJ_\nu(ur)e^{j\nu\phi}e^{j(\omega t - \beta z)} \tag{2-42}$$

$$H_z(r < a) = BJ_\nu(ur)e^{j\nu\phi}e^{j(\omega t - \beta z)} \tag{2-43}$$

where A and B are arbitrary constants.

Outside of the core the solutions to Eq. (2-41) are given by modified Bessel functions of the second kind $K_\nu(wr)$, where $w^2 = \beta^2 - k_2^2$ with

$k_2 = 2\pi n_2/\lambda$. The expressions for E_z and H_z outside the core are therefore

$$E_z(r > a) = CK_\nu(wr)e^{j\nu\phi}e^{j(\omega t-\beta z)} \tag{2-44}$$

$$H_z(r > a) = DK_\nu(wr)e^{j\nu\phi}e^{j(\omega t-\beta z)} \tag{2-45}$$

with C and D being arbitrary constants.

The definition of $J_\nu(ur)$ and $K_\nu(wr)$ and various recursion relations are given in App. C. From the definition of the modified Bessel function, it is seen that $K_\nu(wr) \to e^{-wr}$ as $wr \to \infty$. Since $K_\nu(wr)$ must go to zero as $r \to \infty$, it follows that $w > 0$. This, in turn, implies that $\beta \geq k_2$, which represents a cutoff condition. The *cutoff condition* is the point at which a mode is no longer bound to the core region. A second condition on β can be deduced from the behavior of $J_\nu(ur)$. Inside the core the parameter u must be real for F_1 to be real, from which it follows that $k_1 \geq \beta$. The permissible range of β for bound solutions is therefore

$$n_2 k = k_2 \leq \beta \leq k_1 = n_1 k \tag{2-46}$$

where $k = 2\pi/\lambda$ is the free-space propagation constant.

2.4.4 Modal Equation

The solutions for β must be determined from the boundary conditions. The boundary conditions require that the tangential components E_ϕ and E_z of **E** inside and outside of the dielectric interface at $r = a$ must be the same and similarly for the tangential components H_ϕ and H_z. Consider first the tangential components of **E**. For the z component we have, from Eq. (2-42) at the inner core-cladding boundary ($E_z = E_{z1}$) and from Eq. (2-44) at the outside of the boundary ($E_z = E_{z2}$), that

$$E_{z1} - E_{z2} = AJ_\nu(ua) - CK_\nu(wa) = 0 \tag{2-47}$$

The ϕ component is found from Eq. (2-35*b*). Inside the core the factor q^2 is given by

$$q^2 = u^2 = k_1^2 - \beta^2 \tag{2-48}$$

where $k_1 = 2\pi n_1/\lambda = \omega\sqrt{\epsilon_1\mu}$, while outside the core

$$w^2 = \beta^2 - k_2^2 \tag{2-49}$$

with $k_2 = 2\pi n_2/\lambda = \omega\sqrt{\epsilon_2\mu}$. Substituting Eqs. (2-42) and (2-43) into Eq. (2-35*b*) to find $E_{\phi 1}$, and similarly using Eqs. (2-44) and (2-45) to determine $E_{\phi 2}$, yields at $r = a$

$$E_{\phi 1} - E_{\phi 2} = -\frac{j}{u^2}\left[A\frac{j\nu\beta}{a}J_\nu(ua) - B\omega\mu uJ_\nu'(ua)\right] - \frac{j}{w^2}\left[C\frac{j\nu\beta}{a}K_\nu(wa) - D\omega\mu wK_\nu'(wa)\right] = 0 \tag{2-50}$$

where the prime indicates differentiation with respect to the argument.

Similarly, for the tangential components of **H** it is readily shown that at $r = a$

$$H_{z1} - H_{z2} = BJ_\nu(ua) - DK_\nu(wa) = 0 \tag{2-51}$$

and

$$H_{\phi 1} - H_{\phi 2} = -\frac{j}{u^2}\left[B\frac{j\nu\beta}{a}J_\nu(ua) + A\omega\epsilon_1 uJ_\nu'(ua)\right] - \frac{j}{w^2}\left[D\frac{j\nu\beta}{a}K_\nu(wa) + C\omega\epsilon_2 wK_\nu'(wa)\right] = 0 \tag{2-52}$$

Equations (2-47), (2-50), (2-51), and (2-52) are a set of four equations with four unknown coefficients A, B, C, and D. A solution to these equations exists only if the determinant of these coefficients is zero:

$$\begin{vmatrix} J_\nu(ua) & 0 & -K_\nu(wa) & 0 \\ \frac{\beta\nu}{au^2}J_\nu(ua) & \frac{j\omega\mu}{u}J_\nu'(ua) & \frac{\beta\nu}{aw^2}K_\nu(wa) & \frac{j\omega\mu}{w}K_\nu'(wa) \\ 0 & J_\nu(ua) & 0 & -K_\nu(wa) \\ -\frac{j\omega\epsilon_1}{u}J_\nu'(ua) & \frac{\beta\nu}{au^2}J_\nu(ua) & -\frac{j\omega\epsilon_2}{w}K_\nu'(wa) & \frac{\beta\nu}{aw^2}K_\nu(wa) \end{vmatrix} = 0 \tag{2-53}$$

Evaluation of this determinant yields the following eigenvalue equation for β:

$$(\mathscr{J}_\nu + \mathscr{K}_\nu)(k_1^2\mathscr{J}_\nu + k_2^2\mathscr{K}_\nu) = \left(\frac{\beta\nu}{a}\right)^2\left(\frac{1}{u^2} + \frac{1}{w^2}\right)^2 \tag{2-54}$$

where

$$\mathscr{J}_\nu = \frac{J_\nu'(ua)}{uJ_\nu(ua)} \quad \text{and} \quad \mathscr{K}_\nu = \frac{K_\nu'(wa)}{wK_\nu(wa)}$$

Upon solving Eq. (2-54) for β it will be found that only discrete values restricted to the range given by Eq. (2-46) will be allowed. Although Eq. (2-54) is a complicated transcendental equation which is generally solved by numerical techniques, its solution for any particular mode will provide all the characteristics of that mode. We shall now consider this equation for some of the lowest-order modes of a step index waveguide.

2.4.5 Modes in Step-Index Fibers

To help describe the modes we shall first examine the behavior of the J-type Bessel functions. These are plotted in Fig. 2-16 for the first three orders. The J-type Bessel functions are similar to harmonic functions since they exhibit oscillatory behavior for real k as is the case for sinusoidal functions. Because of the oscillatory behavior of J_ν there will be m roots of Eq. (2-54) for a given ν value. These roots will be designated by $\beta_{\nu m}$, and the corresponding modes are

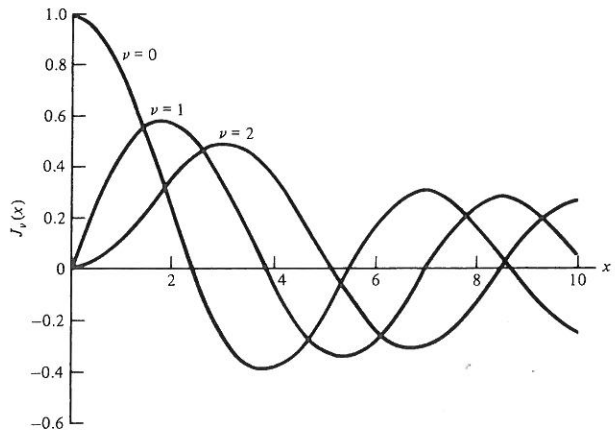

FIGURE 2-16
Variation of the Bessel function $J_\nu(x)$ for the first three orders ($\nu = 0, 1, 2$) plotted as a function of x.

either $TE_{\nu m}$, $TM_{\nu m}$, $EH_{\nu m}$, or $HE_{\nu m}$. Schematics of the transverse electric field patterns for the four lowest-order modes over the cross-section of a step-index fiber are shown in Fig. 2-17.

For the dielectric fiber waveguide all modes are hybrid modes except those for which $\nu = 0$. When $\nu = 0$ the right-hand side of Eq. (2-54) vanishes and two different eigenvalue equations result. These are

$$\mathscr{J}_0 + \mathscr{K}_0 = 0 \tag{2-55a}$$

or, using the relations for J_ν' and K_ν' for App. C,

$$\frac{J_1(ua)}{uJ_0(ua)} + \frac{K_1(wa)}{wK_0(wa)} = 0 \tag{2-55b}$$

which corresponds to TE_{0m} modes ($E_z = 0$), and

$$k_1^2\mathscr{J}_0 + k_2^2\mathscr{K}_0 = 0 \tag{2-56a}$$

or

$$\frac{k_1^2 J_1(ua)}{uJ_0(ua)} + \frac{k_2^2 K_1(wa)}{wK_0(wa)} = 0 \tag{2-56b}$$

which corresponds to TM_{0m} modes ($H_z = 0$). The proof of this is left as an exercise (see Prob. 2-16).

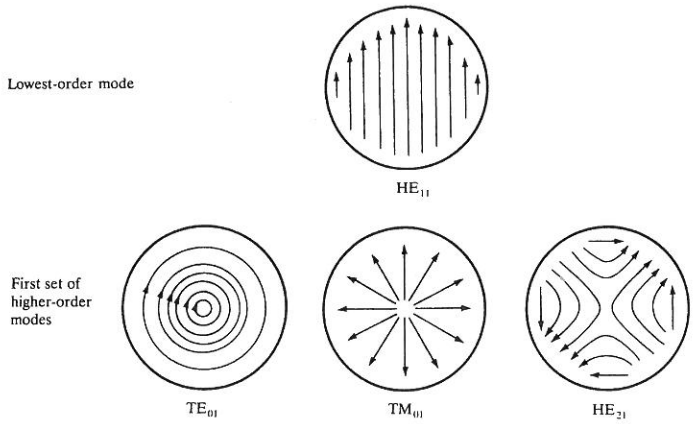

FIGURE 2-17
Cross-sectional views of the transverse electric field vectors for the four lowest-order modes in a step-index fiber.

When $\nu \neq 0$ the situation is more complex and numerical methods are needed to solve Eq. (2-54) exactly. However, simplified and highly accurate approximations based on the principle that the core and cladding refractive indices are nearly the same have been derived by Synder[19] and Gloge.[20,27] The condition that $n_1 - n_2 \ll 1$ was referred to by Gloge as giving rise to *weakly guided* modes. A treatment of these derivations is given in Sec. 2.4.6.

Let us next examine the cutoff conditions for fiber modes. As was mentioned in relation to Eq. (2-46), a mode is referred to as being cut off when it is no longer bound to the core of the fiber, so that its field no longer decays on the outside of the core. The cutoffs for the various modes are found by solving Eq. (2-54) in the limit $w^2 \to 0$. This is, in general, fairly complex, so that only the results,[14,16] which are listed in Table 2-1, will be given here.

TABLE 2-1
Cutoff conditions for some lower-order modes

ν	Mode	Cutoff condition
0	TE_{0m}, TM_{0m}	$J_0(ua) = 0$
1	HE_{1m}, EH_{1m}	$J_1(ua) = 0$
≥ 2	$EH_{\nu m}$	$J_\nu(ua) = 0$
	$HE_{\nu m}$	$\left(\frac{n_1^2}{n_2^2} + 1\right)J_{\nu-1}(ua) = \frac{ua}{\nu - 1}J_\nu(ua)$

An important parameter connected with the cutoff condition is the *normalized frequency* V (also called the *V-number* or *V-parameter*) defined by

$$V^2 = (u^2 + w^2)a^2 = \left(\frac{2\pi a}{\lambda}\right)^2 (n_1^2 - n_2^2) \tag{2-57}$$

which is a dimensionless number that determines how many modes a fiber can support. The number of modes that can exist in a waveguide as a function of V may be conveniently represented in terms of a *normalized propagation constant* b defined by[20]

$$b = \frac{a^2 w^2}{V^2} = \frac{(\beta/k)^2 - n_2^2}{n_1^2 - n_2^2}$$

A plot of b (in terms of β/k) as a function of V is shown in Fig. 2-18 for a few of the low-order modes. This figure shows that each mode can exist only for values of V that exceed a certain limiting value. The modes are cut off when $\beta/k = n_2$. The HE_{11} mode has no cutoff and ceases to exist only when the core diameter is zero. This is the principle on which the single-mode fiber is based. By appropriately choosing a, n_1, and n_2 so that

$$V = \frac{2\pi a}{\lambda}(n_1^2 - n_2^2)^{1/2} \leq 2.405 \tag{2-58}$$

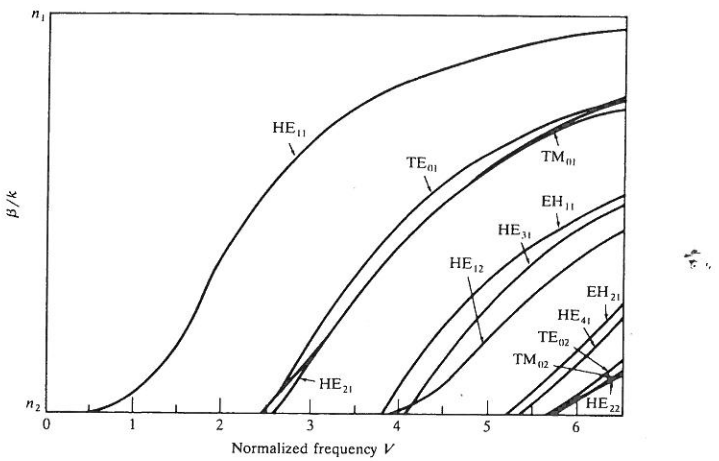

FIGURE 2-18
Plots of the propagation constant (in terms of β/k) as a function of V for a few of the lowest-order modes.

which is the value at which the lowest-order Bessel function J_0 is zero (see Fig. 2-16), all modes except the HE_{11} mode are cut off.

Example 2-3. A step-index fiber has a normalized frequency $V = 26.6$ at a 1300-nm wavelength. If the core radius is 25 μm, let us find the numerical aperture. From Eqs. (2-23) and (2-50) we have

$$V = \frac{2\pi a}{\lambda}\,\text{NA}$$

or

$$\text{NA} = V\frac{\lambda}{2\pi a} = 26.6\frac{1.3}{2\pi(25)} = 0.22$$

The parameter V can also be related to the number of modes M in a multimode fiber when M is large. An approximate relationship for step-index fibers can be derived from ray theory. A ray congruence incident on the end of a fiber will be accepted by the fiber if it lies within an angle θ defined by the numerical aperture as given in Eq. (2-23):

$$\text{NA} = \sin\theta = (n_1^2 - n_2^2)^{1/2} \tag{2-59}$$

For practical numerical apertures $\sin\theta$ is small so that $\sin\theta \simeq \theta$. The solid acceptance angle for the fiber is therefore

$$\Omega = \pi\theta^2 = \pi(n_1^2 - n_2^2) \tag{2-60}$$

For electromagnetic radiation of wavelength λ emanating from a laser or a waveguide the number of modes per unit solid angle is given by $2A/\lambda^2$, where A is the area the mode is leaving or entering.[28] The area A in this case is the core cross section πa^2. The factor 2 comes from the fact that the plane wave can have two polarization orientations. The total number of modes M entering the fiber is thus given by

$$M \simeq \frac{2A}{\lambda^2}\Omega = \frac{2\pi^2 a^2}{\lambda^2}(n_1^2 - n_2^2) = \frac{V^2}{2} \tag{2-61}$$

2.4.6 Linearly Polarized Modes

As may be apparent by now, the exact analysis for the modes of a fiber is mathematically very complex. However, a simpler but highly accurate approximation can be used, based on the principle that in a typical step-index fiber the difference between the indices of refraction of the core and cladding is very small, that is, $\Delta \ll 1$. This is the basis of the *weakly guiding fiber approximation*.[7,19,20,27] In this approximation the electromagnetic field patterns and the propagation constants of the mode pairs $HE_{\nu+1,m}$ and $EH_{\nu-1,m}$ are very similar. This holds likewise for the three modes TE_{0m}, TM_{0m}, and HE_{2m}. This can be seen from Fig. 2-18 with $(\nu, m) = (0, 1)$ and $(2, 1)$ for the mode

groupings $\{HE_{11}\}$, $\{TE_{01}, TM_{01}, HE_{21}\}$, $\{HE_{31}, EH_{11}\}$, $\{HE_{12}\}$, $\{HE_{41}, EH_{21}\}$, and $\{TE_{02}, TM_{02}, HE_{22}\}$. The result is that only four field components need to be considered instead of six, and the field description is further simplified by the use of cartesian instead of cylindrical coordinates.

When $\Delta \ll 1$ we have that $k_1^2 \simeq k_2^2 \simeq \beta^2$. Using these approximations, Eq. (2-54) becomes

$$\mathscr{J}_\nu + \mathscr{K}_\nu = \pm \frac{\nu}{a}\left(\frac{1}{u^2} + \frac{1}{w^2}\right) \tag{2-62}$$

Thus Eq. (2-55*b*) for TE_{0m} modes is the same as Eq. (2-54*b*) for TM_{0m} modes. Using the recurrence relations for J_ν' and K_ν' given in App. C, we get two sets of equations for Eq. (2-62) for the positive and negative signs. The positive sign yields

$$\frac{J_{\nu+1}(ua)}{uJ_\nu(ua)} + \frac{K_{\nu+1}(wa)}{wK_\nu(wa)} = 0 \tag{2-63}$$

The solution of this equation gives a set of modes called the EH modes. For the negative sign in Eq. (2-62) we get

$$\frac{J_{\nu-1}(ua)}{uJ_\nu(ua)} - \frac{K_{\nu-1}(wa)}{wK_\nu(wa)} = 0 \tag{2-64a}$$

or, alternatively, taking the inverse of Eq. (2-64*a*) and using the first expressions for $J_\nu(ua)$ and $K_\nu(wa)$ from Sec. C.1.2 and Sec. C.2.2,

$$-\frac{uJ_{\nu-2}(ua)}{J_{\nu-1}(ua)} = \frac{wK_{\nu-2}(wa)}{K_{\nu-1}(wa)} \tag{2-64b}$$

This results in a set of modes called the HE modes.

If we define a new parameter

$$j = \begin{cases} 1 & \text{for TE and TM modes} \\ \nu + 1 & \text{for EH modes} \\ \nu - 1 & \text{for HE modes} \end{cases} \tag{2-65}$$

then Eqs. (2-55*b*), (2-63), and (2-64*b*) can be written in the unified form

$$\frac{uJ_{j-1}(ua)}{J_j(ua)} = -\frac{wK_{j-1}(wa)}{K_j(wa)} \tag{2-66}$$

Equations (2-65) and (2-66) show that within the weakly guiding approximation all modes characterized by a common set of j and m satisfy the same characteristic equation. This means that these modes are degenerate. Thus, if an $HE_{\nu+1,m}$ mode is degenerate with an $EH_{\nu-1,m}$ mode (that is, if HE and EH modes of corresponding radial order m and equal circumferential order ν form degenerate pairs), then any combination of an $HE_{\nu+1,m}$ mode with an $EH_{\nu-1,m}$ mode will likewise constitute a possible mode of the fiber.

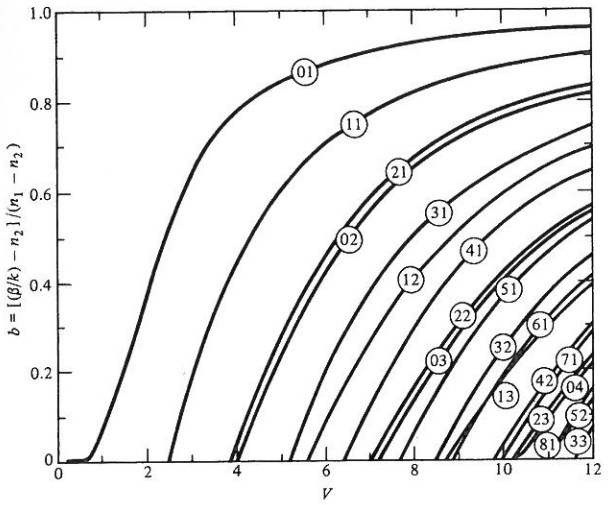

FIGURE 2-19
Plots of the propagation constant b as a function of V for various LP_{jm} modes. (Reproduced with permission from Gloge[20].)

TABLE 2-2
Composition of the lower-order linearly polarized modes

LP-mode designation	Traditional-mode designation and number of modes	Number of degenerate modes
LP_{01}	$HE_{11} \times 2$	2
LP_{11}	$TE_{01}, TM_{01}, HE_{21} \times 2$	4
LP_{21}	$EH_{11} \times 2, HE_{31} \times 2$	4
LP_{02}	$HE_{12} \times 2$	2
LP_{31}	$EH_{21} \times 2, HE_{41} \times 2$	4
LP_{12}	$TE_{02}, TM_{02}, HE_{22} \times 2$	4
LP_{41}	$EH_{31} \times 2, HE_{51} \times 2$	4
LP_{22}	$EH_{12} \times 2, HE_{32} \times 2$	4
LP_{03}	$HE_{13} \times 2$	2
LP_{51}	$EH_{41} \times 2, HE_{61} \times 2$	4

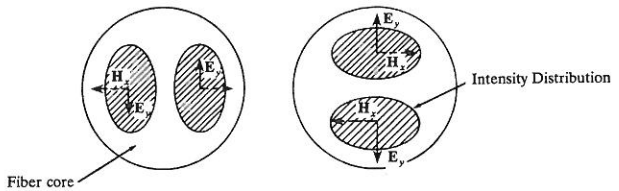

FIGURE 2-20
The four possible transverse electric field and magnetic field directions and the corresponding intensity distributions for the LP_{11} mode.

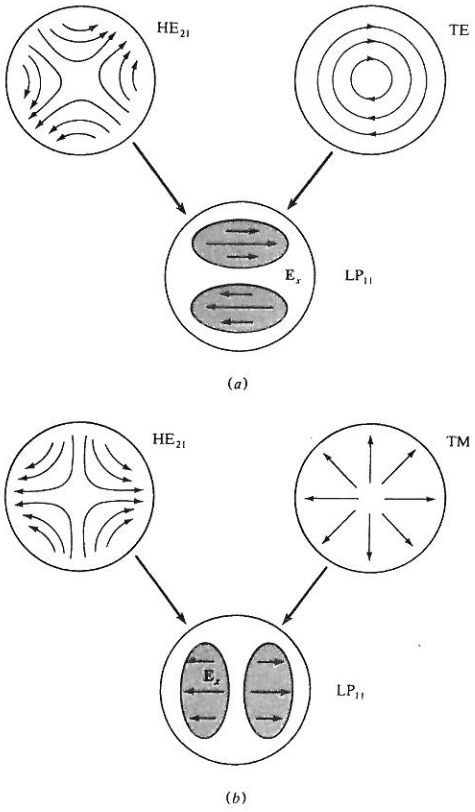

FIGURE 2-21
Composition of two LP_{11} modes from exact modes and their transverse electric field and intensity distributions.

Gloge[20] proposed that such degenerate modes be called *linearly polarized* (LP) modes, and be designated LP_{jm} modes regardless of their TM, TE, EH, or HE field configuration. The normalized propagation constant b as a function of V is given for various LP_{jm} modes in Fig. 2-19. In general we have the following:

1. each LP_{0m} mode is derived from an HE_{1m} mode;
2. each LP_{1m} mode comes from TE_{0m}, TM_{0m}, and HE_{2m} modes;
3. each $LP_{\nu m}$ mode ($\nu \geq 2$) is from an $HE_{\nu+1,m}$ and an $EH_{\nu-1,m}$ mode.

The correspondence between the ten lowest LP modes (that is, those having the lowest cutoff frequencies) and the traditional TM, TE, EH, and HE modes is given in Table 2-2. This table also shows the number of degenerate modes.

A very useful feature of the LP-mode designation is the ability to readily visualize a mode. In a complete set of modes only one electric and one magnetic field component are significant. The electric field vector **E** can be chosen to lie along an arbitrary axis, with the magnetic field vector **H** being perpendicular to it. In addition there are equivalent solutions with the field polarities reversed. Since each of the two possible polarization directions can be coupled with either a cos $j\phi$ or a sin $j\phi$ azimuthal dependence, four discrete mode patterns can be obtained from a single LP_{jm} label. As an example, the four possible electric and magnetic field directions and the corresponding intensity distributions for the LP_{11} mode are shown in Fig. 2-20. Figures 2-21*a* and 2-21*b* illustrate how two LP_{11} modes are composed from the exact HE_{21} plus TE_{01} and the exact HE_{21} plus TM_{01} modes, respectively.

2.4.7 Power Flow in Step-Index Fibers

A final quantity of interest for step-index fibers is the fractional power flow in the core and cladding for a given mode. As is illustrated in Fig. 2-14, the electromagnetic field for a given mode does not go to zero at the core-cladding interface, but changes from an oscillating form in the core to an exponential decay in the cladding. Thus the electromagnetic energy of a guided mode is carried partly in the core and partly in the cladding. The further away a mode is from its cutoff frequency the more concentrated its energy is in the core. As cutoff is approached, the field penetrates further into the cladding region and a greater percentage of the energy travels in the cladding. At cutoff the field no longer decays outside the core and the mode now becomes a fully radiating mode.

The relative amounts of power flowing in the core and the cladding can be obtained by integrating the Poynting vector in the axial direction,

$$S_z = \tfrac{1}{2}\,\mathrm{Re}(\mathbf{E} \times \mathbf{H}^*) \cdot \mathbf{e}_z \qquad (2\text{-}67)$$